

Direct graphene synthesis on SiO₂/Si substrate by ion implantation

R. Zhang, Z. S. Wang, Z. D. Zhang, Z. G. Dai, L. L. Wang, H. Li, L. Zhou, Y. X. Shang, J. He, D. J. Fu, and J. R. Liu

Citation: [Applied Physics Letters](#) **102**, 193102 (2013); doi: 10.1063/1.4804982

View online: <http://dx.doi.org/10.1063/1.4804982>

View Table of Contents: <http://scitation.aip.org/content/aip/journal/apl/102/19?ver=pdfcov>

Published by the [AIP Publishing](#)

Articles you may be interested in

[Drawing graphene nanoribbons on SiC by ion implantation](#)

Appl. Phys. Lett. **100**, 073501 (2012); 10.1063/1.3682479

[Graphene synthesis by ion implantation](#)

Appl. Phys. Lett. **97**, 183103 (2010); 10.1063/1.3507287

[Ion beam synthesis of cubic-SiC layer on Si\(111\) substrate](#)

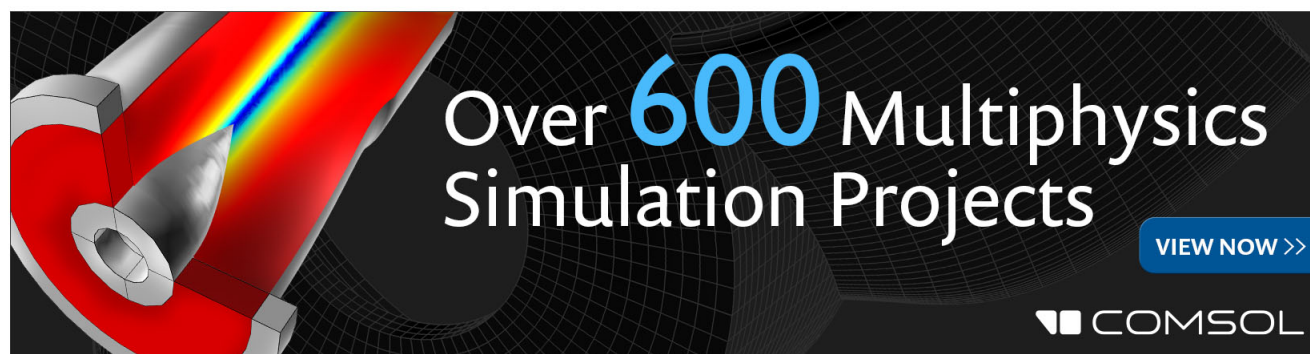
J. Appl. Phys. **100**, 063504 (2006); 10.1063/1.2344813

[Ion-implantation-prepared catalyst nanoparticles for growth of carbon nanotubes](#)

Appl. Phys. Lett. **86**, 053104 (2005); 10.1063/1.1856699

[Structural inhomogeneity and silicon enrichment of buried SiO₂ layers formed by oxygen ion implantation in silicon](#)

J. Appl. Phys. **82**, 2184 (1997); 10.1063/1.366025

The advertisement for COMSOL Multiphysics features a 3D rendering of a mechanical part with a colorful stress or temperature distribution. The text 'Over 600 Multiphysics Simulation Projects' is prominently displayed in white and blue. A blue button with the text 'VIEW NOW >>' is located on the right. The COMSOL logo is in the bottom right corner.

Over 600 Multiphysics Simulation Projects

[VIEW NOW >>](#)

COMSOL



Direct graphene synthesis on SiO₂/Si substrate by ion implantation

R. Zhang,¹ Z. S. Wang,¹ Z. D. Zhang,¹ Z. G. Dai,¹ L. L. Wang,¹ H. Li,¹ L. Zhou,¹
Y. X. Shang,¹ J. He,² D. J. Fu,^{1,a)} and J. R. Liu^{3,b)}

¹Key Laboratory of Artificial Micro- and Nano-Materials of Ministry of Education and Accelerator Laboratory, School of Physics and Technology, Wuhan University, 430072 Wuhan, China

²Division for Accelerators, Institute of High Energy of Physics, Chinese Academy of Sciences, 19B Yuquan Rd., Shijingshan District, Beijing 100049, China

³Texas Center for Superconductivity, University of Houston, 4800 Calhoun Road, Houston, Texas 77004, USA

(Received 2 February 2013; accepted 23 April 2013; published online 13 May 2013)

We present results of few-layer graphene synthesis directly on SiO₂/Si substrate by negative carbon ion implantation in Ni catalyst films on the top of SiO₂/Si substrate. Negative carbon ions at 20 keV were implanted into Ni films with doses of $(4\text{--}16) \times 10^{15} \text{ cm}^{-2}$. The implanted carbon atoms dissolved in Ni at an elevated temperature and diffused towards both sides of the Ni film. After annealing, graphene layers were observed on top of the Ni surface and on SiO₂ beneath the Ni film. Formation of graphene layers directly on insulating substrates was achieved by etching the top Ni layer. © 2013 AIP Publishing LLC. [<http://dx.doi.org/10.1063/1.4804982>]

Graphene, the two-dimensional sp² carbon atoms structure, has a promising prospect of applications due to its fascinating physical and electrical properties, such as high carrier mobility up to $200\,000 \text{ cm}^2 \text{ V}^{-1} \text{ s}^{-1}$ at 4 K for the single layer graphene¹ and perfect optical transparency.² During last few years, many approaches for graphene synthesis have been reported, such as mechanical exfoliation from graphite,^{1,3,4} epitaxial growth on crystalline substrate.^{5,6} One of the most popular techniques, chemical vapor deposition (CVD), allowed successful production of large scale graphene layers.^{7,8} The successful production of large area graphene layers greatly encouraged the graphene applications in micro-electronic devices. Some pioneers in this area are talking on replacing silicon by graphene. Unfortunately, in large area CVD graphene production, it is necessary to transfer the as-grown graphene onto desired substrates, such as SiO₂ on silicon. The wet-transfer process is incompatible with existing mature Si-processing technologies and may cause additional graphene degradation. Therefore, processes for production of graphene layers on desirable functional materials, such as insulators like SiO₂/Si and Al₂O₃ or Si, without transferring, attract great attention. Recently, there are some reports on direct graphene growth on insulator substrate, such as SiO₂,^{9,10} h-BN,¹¹ and Co₃O₄.³ Among them, a variety of techniques for direct graphene synthesis on SiO₂ are more attractive for future device applications.^{4–6,9–13} In this direction, one of the most promising and mature technique in micro-electronic device fabrication, namely, ion implantation, has not been reported yet. Ion implantation as a compatible technique with existing Si-processing technologies shows some essential advantages. First, in ion implantation, the amount of implanted C atoms corresponding to the graphene layer thickness is controlled by the implanted dose with accuracy up to 1%–2%, which is the best controllable process.

Second, present Si-processing for large scale micro-electronic fabrication with wafer-size up to 12 in. ion implantation is a mature technique with the uniformity of 1%–2%. Recently, it was reported that ion implantation technique was used to grow uniform and large area graphene as well as improved graphene layers by carbon ions in Ni thin films.^{14–17} The mechanism of direct graphene growth by CVD on the insulating substrate and tendency to bilayer graphene films between the metal film and the substrate is not well clear. As a controllable tool on carbon content, ion implantation has a potential to provide a delicated interpretation on these issues.

In this letter, we report transfer-free synthesis of graphene layers on SiO₂/Si substrates by ion implantation at room temperature. The carbon atoms in the implanted region dissolved into Ni at an elevated temperature and diffused towards both sides of the Ni films. Thin Ni film (300 nm) was chosen as a starting material for catalyzing graphene growth and was evaporated on SiO₂/Si substrates by e-beam evaporator. The grain sizes of as-deposited and C-implanted Ni films both are 30 nm in average. Negative carbon atoms were implanted into Ni films with the energy of 20 keV for a variety of dosages. SRIM (Stopping and Range of Ion in Matter) calculations show that the projected range of 20 keV carbon ions in Ni is about 24 nm with the longitudinal straggling about 19 nm.¹⁶ In order to minimize the contamination, the vacuum was kept in 10^{-3} Pa during the implantation process. Afterwards, *ex-situ* annealing treatment was conducted at 900 °C in vacuum ambient for 50 min and then cooled the sample down to room temperature with a cooling rate of 20 °C/min. We observed the graphene layer on the top of Ni films. To avoid the top surface graphene dropping on the SiO₂/Si substrates, we applied O₂ plasma on the Ni surface to remove the carbon materials before etching the Ni films. Subsequently, the Ni thin films were dissolved by aqueous HCl solution and the resulting graphene/SiO₂ was rinsed with deionized water. Afterwards, we investigated graphene layers on SiO₂/Si substrate for various ion implantation dosages. The graphene on the top of Ni and SiO₂/Si substrate was investigated by a micro-Raman spectrometer (LabRAM

^{a)} Author to whom correspondence should be addressed. Electronic mail: djfu@whu.edu.cn.

^{b)} Retired from Texas Center for Superconductivity, University of Houston, 4800 Calhoun Road, Houston, Texas 77004, USA.

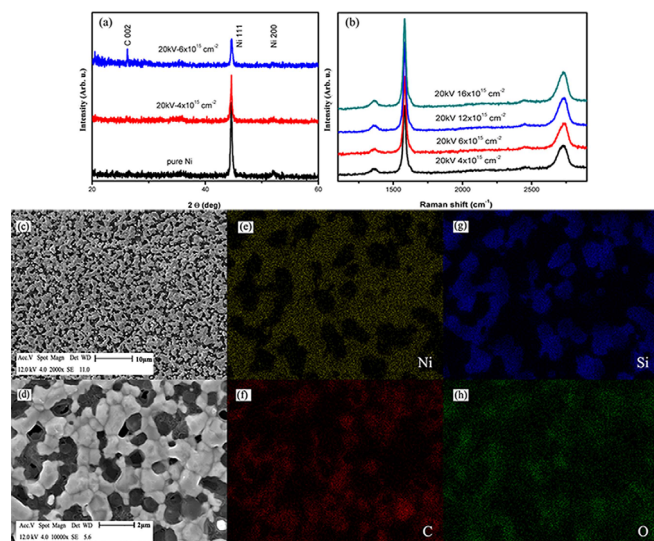


FIG. 1. (a) XRD spectra of Ni films implanted with various ion fluences; (b) graphene on Ni surface; (c) SEM images of the graphene surface on Ni implanted with 12×10^{15} C-atoms/cm²; (e)–(h) EDS mapping for Ni, Si, C, and O elements in the region shown in (d).

HR800) with the excited wavelength of 488 nm at a power of 10 mW.

Fig. 1(a) shows X-ray diffraction (XRD) spectra of pure Ni and C ion implanted Ni films with a variety of C ion doses. The intensities of the Ni (111) and Ni (200) peaks decrease with increasing ion dosages, which indicate that the polycrystalline structure of Ni films has been damaged at the dose of 6×10^{15} cm⁻² but remains the relatively overall good structure after implantation process. The characteristic C (002) peak at 26.3° is attributed to carbon in the depth of ion projected range in Ni films and the corresponding d-spacing is 0.34 nm. The strongest diffraction peak of C (002) appears at the highest implanted dose of 6×10^{15} cm⁻², which supplied by the carbon implanted region.¹⁸ The implanted Ni films were annealed at 900 °C and followed by cooling for C atoms to segregate and precipitate. The Raman spectra of graphene-on-nickel with selected carbon doses are shown in Fig. 1(b). The Raman peaks at 1350 cm⁻¹ (D band), 1580 cm⁻¹ (G band), and 2720 cm⁻¹ (2D band) are showing few-layer graphene on top of the Ni films for different C implantation dosages. The G band is associated with the in-plane sp^2 carbon atom vibration and with the doubly degenerate phonon E_{2g} mode at the Brillouin zone center. The 2D band originates from second-order scattering

by two phonon resonance. The presence of D band from the first-order scattering by zone-boundary phonons means there are structural disorder or defects.

Fig. 1(c) shows a scanning electron microscopy (SEM) image taken at 12 kV, revealing morphology of graphene on the top of Ni film implanted with carbon ions to 12×10^{15} cm⁻². Fig. 1(d) is a magnified image of Fig. 1(c). To study the origin of the graphene on Ni, EDX measurement was conducted to find the distribution of Ni, carbon, and SiO₂ substrate, as shown in Figs. 1(e)–1(h), respectively. Abundant carbon atoms are found on island-like nickel grains, which is complementary with substrate elements. The few-layer graphene films are mostly formed from the grain boundaries. During annealing, part of Ni atoms have redistributed and SiO₂ has remained.⁹ The carbon atoms diffuse and segregate at the Ni surface to form graphene, especially few-layer graphene around the Ni grains which have accumulated excessive carbon atoms and acted as nucleation sites.

To confirm the graphene growth on SiO₂/Si but not the graphene flakes from the top of Ni surface, a controlled experiment by O₂ plasma etching was carried out and the Raman spectra with dosage of 4×10^{15} cm⁻² are shown in Fig. 2(a). The red curve shows the graphene growth on the nickel surface after annealing the C ion implanted Ni/SiO₂/Si samples, revealing a small D peak with an intensity ratio of I_D/I_G around 0.3. After O₂ plasma treatment for 50 min, the surface graphene on top of Ni has been completely removed, as shown by the black curve, which does not show any Raman peaks for carbon allotropes. After etching the Ni layers, the blue curve shows the graphene on SiO₂/Si substrate as a few-layer graphene film with its 2D peak at 2728 cm⁻¹ and $I_G/I_{2D} \sim 1.7$. The full width at high maximum (FWHM) was determined after subtracting the baseline and searching peak position by using Raman peak fitting program. The graphene on SiO₂ shows FWHM of the 2D peak as 75 cm⁻¹, which is broader than graphene on top of the Ni surface before the plasma etching (about 46 cm⁻¹). At the same time, the D peak increases up to a ratio $I_D/I_G \sim 0.5$, implying the presence of more disorders or defects. The higher disorders may be caused by the insufficient implanted carbon dosage to form graphene on two sides of Ni film and/or the contaminant due to etching process. The SEM image in Fig. 2(b) shows that graphene on SiO₂/Si with the implanted dosage of 4×10^{15} cm⁻² has a relatively flat surface with corrugation appearance.

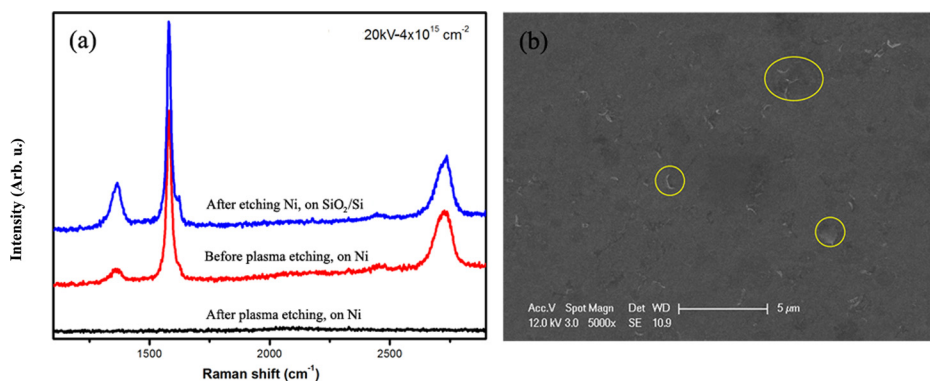


FIG. 2. (a) Raman spectra of graphene on the top of Ni layer before and after O₂ plasma etching, and graphene on SiO₂/Si after removing Ni; (b) SEM image of graphene on SiO₂/Si substrate. The ion dose of the samples is 4×10^{15} cm⁻².

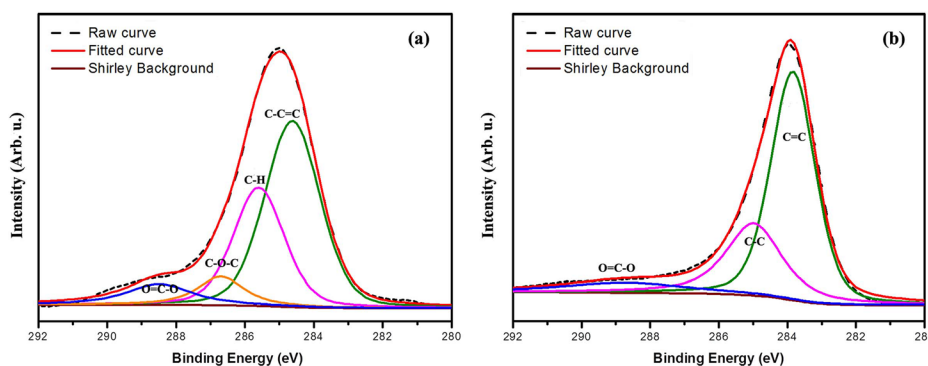


FIG. 3. XPS spectra of graphene on SiO_2 and Ni surfaces.

X-ray photoelectron spectroscopy (XPS) is used for the surface information such as elemental species identification and chemical state analysis. It was carried out by KRATOS XSAM800 X-ray photoelectron spectroscopy with Mg $K\alpha$ radiation of 1253.6 eV as the excitation source in a ultra-high vacuum system at 6×10^{-7} Pa. The full scan of XPS spectrum of graphene/ SiO_2 substrate for C-implanted sample up to $4 \times 10^{15} \text{ cm}^{-2}$ reveals the presence of C, Si, and O. The Si and O elements mainly originate from the substrate since the implantation and annealing processes were conducted in vacuum. To further investigate the graphene chemical bonds, the C 1s line has been deconvoluted into four component peaks, as shown in Fig. 3(a). The dominant peak located at 284.6 eV (C-C=C) is corresponding to sp^2 bonding. The C 1s spectrum exhibits an asymmetric shoulder at a higher binding energy, which is representative of defective states of sp^3 hybridization with C-O or C=O chemical bonds, located at 285.6 eV (C-H or C-OH), 286.7 eV (C-O-C), and 288.5 eV (O=C-O), respectively.^{7,19–24} Nickel related features were not observed in the XPS full-scan spectrum, indicating that Ni has been removed completely. Hydrogen from HCl contamination and oxygen from water molecules induce sp^3 carbon bonding and affect the spectral line shape. For comparison, a C 1s core level spectrum of graphene/Ni is shown in Fig. 3(b). It is deconvoluted into three constituent peaks, and we find that the graphene on the Ni surface has a higher C-C sp^2 binding energy but lower C-H and O=C-O sp^3 binding energies.

Since the implantation dosages are nominally decided amounts, the number of graphene layers can be ensured by controlling the amount of implanted carbon atoms. However, Mun *et al.* reported that at a given implanted dosage the number of graphene layers was seriously influenced by the annealing process.¹⁵ If the implanted samples were heated in the furnace, the segregated carbon atom as nucleation sites would stimulate the Ni surface to absorb residual carbon from the furnace to regrow the graphene. Compared with CVD method, the ion implantation technique has the advantage for controlling the thickness of graphene by tuning ion dosages. Theoretically, the precipitation and segregation of carbon atoms are strongly influenced by the annealing process. So the thickness of graphene layers, to some degree, is not controlled by the implanted number of carbon atoms only, even for the uniform precipitating process, but also by the annealing process.

It is known that in CVD method for graphene growth, there are two processes: the carbon atoms solute into the nickel films from external C source and the catalyzed atoms segregation at the surface to form graphene. In ion

implantation technique for graphene synthesis, the carbon atoms are implanted by energetic ions as a non-equilibrium process without the solid solubility limitation. When the temperature is elevated on implanted specimen, the buried carbon atoms will dissolve into Ni films as solid solution.

Fig. 4(a) shows Raman spectra of graphene/ SiO_2 as a function of dosages. When the dosage increases up to $1.6 \times 10^{16} \text{ cm}^{-2}$, the intensity of 2D peak is decreased, implying the multilayer graphene film. The D peak related to the defects is increased. Carbon atoms implanted into a metal at a high dose will cause pressure in the same order of magnitude for inter gas in noble metals.²⁵ Graphitization taking place at the metal surface forms bubble-like graphene on Ni surface at 20 keV- $1.6 \times 10^{16} \text{ cm}^{-2}$ (not shown here). The SEM observation for graphene/ SiO_2 /Si with the $1.6 \times 10^{16} \text{ cm}^{-2}$ carbon implantation shows some patch-like graphene layers on the SiO_2 surface. The graphitization in the high dose carbon implanted Ni film causes volume expansion and creates restrictive environment at the interface between Ni and SiO_2 . Moreover, there may be some particles on the surface coming from the wet-etching process as defects corresponding to the high D peak in Raman spectra of graphene on SiO_2 in Fig. 4(a).

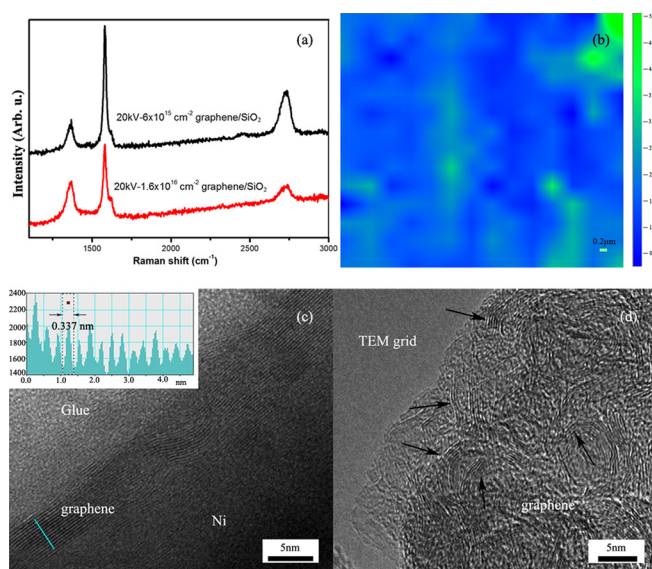


FIG. 4. (a) Raman spectra of graphene on SiO_2 ; the ion doses are $6 \times 10^{15} \text{ cm}^{-2}$ for (b) and $1.6 \times 10^{16} \text{ cm}^{-2}$ for (c) and (d); (b) Raman intensity ratio mapping of G/D over $2.8 \times 2.8 \mu\text{m}^2$; (c) cross-section HRTEM image of graphene on Ni surface; and (d) plan view HRTEM image of graphene flakes directly grown SiO_2 .

Shown in Fig. 4(b) is the color-coded intensity ratio mapping of G/D with the dosage of $6 \times 10^{15} \text{ cm}^{-2}$ over $2.8 \times 2.8 \mu\text{m}^2$.

High resolution transmission electron microscopy (HRTEM) using JEOL JEM-2010 observation was conducted to graphene films on Ni surface and insulating substrates. The cross-section HRTEM view in Fig. 4(c) shows clear multi-layer graphene on the Ni surface at the dosage of $1.6 \times 10^{16} \text{ cm}^{-2}$. The graphene films formed directly on SiO_2/Si were transferred to micro-grids for plan-view HRTEM as shown in Fig. 4(d). The wrinkles allow us to count the number of graphene layers from bilayer to six layers at this selected region.

In conclusion, graphene layers were synthesized on SiO_2/Si substrates by the ion implantation method. Negative ions of carbon at 20 keV with a series of dosages were implanted into Ni films on SiO_2/Si substrates at room temperature. Graphene layers were formed at both sides of the Ni films after annealing processes, and graphene with sp^2 structure was confirmed by Raman spectroscopy. After etching the Ni layer, graphene has been formed directly on the SiO_2/Si substrates. Theoretically, any appropriate functional materials, such as sapphire and BN, can be used as substrates to synthesize graphene on them directly by ion implantation method. Ion implantation provides a controllable carbon source to Ni films, which gives an interpretation on graphene synthesized between Ni and insulating substrates. Diffusion of carbon atoms along grain boundaries is an anisotropic process and favorable for the segregation sites which are inclined to form multi-layer graphene. When epitaxial Ni films are used as catalysts, the layer thickness and uniformity will be improved.²⁶ Ion implantation provides a promising technique for large scale fabrication of hybrid devices with graphene on insulating substrates.

This work was supported by NSFC under grant 11205116, the International Program of the Ministry of Science and Technology of China under 2010DFA02010 and 2011DFR50580 and the Fundamental Research Funds (20102020200034) for the Central Universities.

¹K. S. Novoselov, A. K. Geim, S. V. Morozov, D. Jiang, Y. Zhang, S. V. Dubonos, I. V. Grigorieva, and A. A. Firsov, *Science* **306**, 666 (2004).

- ²S. Bae, H. Kim, Y. Lee, X. F. Xu, J. S. Park, Y. Zheng, J. Balakrishnan, T. Lei, H. R. Kim, Y. I. Song *et al.*, *Nat. Nanotechnol.* **5**, 574 (2010).
- ³M. Zhou, F. L. Pasquale, P. A. Dowben, A. Boosalis, M. Schubert, V. Darakchieva, R. Yakimova, L. Kong, and J. A. Kelber, *J. Phys.: Condens. Matter* **24**, 072201 (2012).
- ⁴D. Kang, W. J. Kim, J. A. Lim, and Y. W. Song, *ACS Appl. Mater. Interfaces* **4**, 3663 (2012).
- ⁵H. J. Shin, W. M. Choi, S. M. Yoon, G. H. Han, Y. S. Woo, E. S. Kim, S. J. Chae, X. S. Li, A. Benayad, D. D. Loc, F. Gunes, Y. H. Lee, and J. Y. Choi, *Adv. Mater.* **23**, 4392 (2011).
- ⁶Z. Peng, Z. Yan, Z. Sun, J. Yao, Y. Zhu, Z. Liu, P. M. Ajayan, and J. M. Tour, *ACS Nano* **5**, 8187 (2011).
- ⁷L. Ci, L. Song, C. Jin, D. Jariwala, D. Wu, Y. Li, A. Srivastava, Z. F. Wang, K. Storr, L. Balicas, F. Liu, and P. M. Ajayan, *Nature Mater.* **9**, 430 (2010).
- ⁸A. Reina, X. Jia, J. Ho, D. Nezich, H. Son, V. Bulovic, M. S. Dresselhaus, and J. Kong, *Nano Lett.* **9**, 30 (2009).
- ⁹T. Kato and R. Hatakeyama, *ACS Nano* **6**, 8508 (2012).
- ¹⁰S. Lizzit, R. Larciprete, P. Lacovig, M. Dalmiglio, F. Orlando, A. Baraldi, L. Gammelgaard, L. Barreto, M. Bianchi, E. Perkins, and P. Hofmann, *Nano Lett.* **12**, 4503 (2012).
- ¹¹Z. Liu, L. Song, S. Zhao, J. Huang, L. Ma, J. Zhang, J. Lou, and P. M. Ajayan, *Nano Lett.* **11**, 2032 (2011).
- ¹²Z. Yan Z. Peng, Z. Sun, and J. M. Tour, *ACS Nano* **5**, 8241 (2011).
- ¹³A. Ismach, C. Druzgalski, S. Penwell, A. Schwartzberg, M. Zheng, A. Javey, J. Bokor, and Y. G. Zhang, *Nano Lett.* **10**, 1542 (2010).
- ¹⁴S. Garaj, W. Hubbard, and J. A. Golovchenko, *Appl. Phys. Lett.* **97**, 183103 (2010).
- ¹⁵L. Baraton, Z. He, C. S. Lee, J. L. Maurice, C. S. Cojocaru, A. F. Gourgues-Lorenzon, Y. H. Lee, and D. Pribat, *Nanotechnology* **22**, 085601 (2011).
- ¹⁶R. Zhang, Z. D. Zhang, Z. S. Wang, S. X. Wang, W. Wang, D. Fu, and J. Liu, *Appl. Phys. Lett.* **101**, 011905 (2012).
- ¹⁷J. H. Mun, S. K. Lim, and B. J. Cho, *J. Electrochem. Soc.* **159**, G89 (2012).
- ¹⁸J. F. Ziegler, M. D. Ziegler, and J. P. Biersack, *Nucl. Instrum. Methods Phys Res. B* **268**, 1818 (2010).
- ¹⁹S. T. Lee, S. Chen, G. Braunstein, X. Feng, I. Bello, and W. M. Lau, *Appl. Phys. Lett.* **59**, 785 (1991).
- ²⁰A. K. Ray, R. K. Sahu, V. Rajinikanth, H. Bapari, M. Ghosh, and P. Paul, *Carbon* **50**, 4123 (2012).
- ²¹M. J. Webb, P. Palmgren, P. Pal, O. Karis, and H. Grennberg, *Carbon* **49**, 3242 (2011).
- ²²V. Datsyuk, M. Kalyva, K. Papagelis, J. Parthenios, D. Tasis, A. Siokou, I. Kallitsis, and C. Galiotis, *Carbon* **46**, 833 (2008).
- ²³J. T. Chen, G. A. Zhang, B. M. Luo, D. F. Sun, X. B. Yan, and Q. J. Xue, *Carbon* **49**, 3141 (2011).
- ²⁴N. Peltekis, S. Kumar, N. McEvoy, K. H. Lee, A. Weidlich, and G. S. Duesberg, *Carbon* **50**, 395 (2012).
- ²⁵Z. H. Zhang, L. Chow, K. Paschke, N. Yu, Y. K. Tao, K. Matsuishi, R. L. Meng, P. Hor, and W. K. Chu, *Appl. Phys. Lett.* **61**, 2650 (1992).
- ²⁶Y. Zhang, L. Gomez F. N. Ishikawa, A. Madaria, K. Ryu, C. Wang, A. Badmaev, and C. Zhou, *J. Phys. Chem. Lett.* **1**, 3101 (2010).